The bouquet of grapevine (*Vitis vinifera* L. cv. Cabernet Sauvignon) flowers arises from the biosynthesis of sesquiterpene volatiles in pollen grains

Diane M. Martin[a,b], Omid Toub[a,b], Angela Chiang[b], Bernard C. Lo[a,b], Sebastian Ohse[a,b], Steven T. Lund[b], and Jörg Bohlmann[a,b,1]

[a]Michael Smith Laboratories and [b]Wine Research Centre, University of British Columbia, Vancouver, BC, Canada V6T 1Z4

Edited by Richard A. Dixon, The Samuel Roberts Noble Foundation, Ardmore, OK, and approved March 11, 2009 (received for review February 6, 2009)

Terpenoid volatiles are important information molecules that enable pollinators to locate flowers and may protect reproductive tissues against pathogens or herbivores. Inflorescences of grapevine (*Vitis vinifera* L.) are composed of tiny green flowers that produce an abundance of sesquiterpenoid volatiles. We demonstrate that male flower parts of grapevines are responsible for sesquiterpenoid floral scent formation. We describe temporal and spatial patterns of biosynthesis and release of floral volatiles throughout the blooming of *V. vinifera* L. cv. Cabernet Sauvignon. The biosynthesis of sesquiterpene volatiles, which are emitted with a light-dependent diurnal pattern early in the morning at prebloom and bloom, is localized to anthers and, more specifically, within the developing pollen grains. Valencene synthase (VvValCS) enzyme activity, which produces the major sesquiterpene volatiles of grapevine flowers, is present in anthers. *VvValCS* transcripts are most abundant in flowers at prebloom stages. Western blot analysis identified VvValCS protein in anthers, and in situ immunolabeling located VvValCS protein in pollen grains during bloom. Histochemical staining, as well as immunolabeling analysis by fluorescent microscopy and transmission electron microscopy, indicated that VvValCS localizes close to lipid bodies within the maturing microspore.

anthers | floral scent | flower development | sesquiterpenes | terpenoid biosynthesis

Although the release of volatiles, including aliphatics, terpenoids, and phenylpropanoids, from anthers and/or pollen has been reported (1), the molecular mechanisms and localization of pollen volatile formation remain uncertain. Pollen volatiles serve as attractants for pollinators and also may function to deter herbivores and defend against pathogens (2). They can be distinct from the scents of other floral organs and may decrease after pollination, thereby advertising the pollen of unvisited flowers to pollinators (1, 3). Pollen volatiles are thought to be localized to the pollenkitt, a waxy substance localized to the grooves in the exine, which provides protection against pathogens, desiccation, or UV light and assists in pollen–pistil interactions (1, 4). Various nonvolatile compounds of the pollenkitt and sporopollenin are deposited on the surface of microspores by tapetum cells (4). Although it has been postulated that the tapetum also produces volatiles (1, 5), this has not been established experimentally.

Grapevines produce dense panicles of small flowers with tiny petals fused into a cap (Fig. 1). Most cultivated grapevines have perfect hermaphroditic flowers and are thought to be at least partially autogamous or cleistogamous (6), whereas their wild relatives are dioecious and have functionally pistillate or staminate flowers that require insect pollinators for fertilization (7, 8). The composition of floral volatiles of several cultivated grapevine varieties has been described (9–11), but little else is known about the molecular biochemistry of grapevine floral scent. Research over the last 15 years in only a few plant species (e.g., *Clarkia breweri*, snapdragon, tobacco, *Arabidopsis*, roses) provides the bulk of information regarding the regulation and biosynthesis of flower volatiles, with a focus of floral scent emissions from the petals and stigma of showy flowers (12). Transcript profiling in *Arabidopsis* and *Magnolia grandiflora* found the expression of sesquiterpene synthases in anthers (13, 14), suggesting a role for male flower organs in the biosynthesis of floral volatiles.

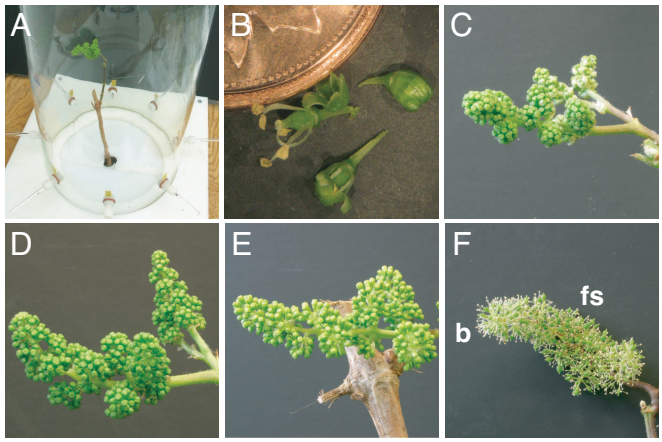

Fig. 1. Flower development on rooted cuttings of grapevine (*V. vinifera* L. cv. Cabernet Sauvignon) used for headspace volatile collection. (*A*) Flower panicle (top node) of a rooted cane inside the volatile collection chamber. The lateral vine (lower node) is below the chamber (not shown). (*B*) Individual flowers clockwise from top right at stage VI, just opening, and in bloom. A penny is used as a scale reference. (*C*) Stage IV flowers; the flowers are separated from one another. (*D*) Stage V flowers; the flowers are lengthened. (*E*) Stage VI flowers; just before bloom, when the flowers are lengthened. (*F*) Flowers at bloom (b) and at fruit set (fs) several days after bloom are identified by a swelling of the pistil.

Here we describe the qualitative and quantitative composition and the spatial, temporal, and developmental patterns of the biosynthesis and release of *Vitis vinifera* L. cv. Cabernet Sauvignon floral sesquiterpene volatiles. Anthers are identified as the floral organ with the highest levels of sesquiterpene volatiles immediately before bloom and at bloom. These volatiles seem to

Author contributions: D.M.M. and J.B. designed research; D.M.M., O.T., A.C., B.C.L., and S.O. performed research; S.T.L. contributed new reagents/analytic tools; D.M.M., O.T., A.C., B.C.L., and S.O. analyzed data; and D.M.M. and J.B. wrote the paper.

The authors declare no conflict of interest.

This article is a PNAS Direct Submission.

Data deposition: The sequence reported in this paper has been deposited in the GenBank database (accession no. FJ696653).

[1]To whom correspondence should be addressed. E-mail: bohlmann@msl.ubc.ca.

This article contains supporting information online at www.pnas.org/cgi/content/full/0901387106/DCSupplemental.

be localized initially within the pollen grain and later within and outside of the pollen grain. The sesquiterpene synthase VvValCS produces the majority of sesquiterpene pollen volatiles in the male flower parts. This work provides fundamental new information about the biosynthesis and localization of terpenoid volatiles in anthers and the developing pollen grains.

Results

Grapevine Flowers Release Bursts of Sesquiterpene Volatiles in the Morning. We collected flower volatiles prebloom and throughout bloom from inflorescences of the first or second node from the top of rooted grapevine (*V. vinifera* L. cv. Cabernet Sauvignon) cuttings (Fig. 1*A*). Leaves from a lateral shoot of a lower node were kept outside of the headspace collection system. During bloom, volatiles were emitted with a maximum of up to 1,047 (± 504) pg/flower/h, primarily in the morning between 0600 and 1100 hours, which coincided with the beginning of the light period [Fig. 2A and supporting information (SI) Fig. S1*A*]. The relatively large variation in the amounts of emissions detected for a given time point likely is due to the fact that opening of flowers within a cluster is not synchronized and varies between clusters. The release of volatiles between 0600 and 1100 hours remained elevated over a period of 3–5 days while individual flowers of a given cluster continued to open. The largest amount of volatiles was released during two 1-h sampling periods between 0600 and 0800 hours (Fig. 2*A*). During the time of maximum volatile release, sesquiterpenes composed up to 86% of total emissions, whereas aliphatic compounds composed up to 16% of total emissions (Fig. S1*B*, Table S1). The sesquiterpenes (+)-valencene, E,E-α-farnesene, and (-)-7-*epi*-α-selinene were the most prominent, with up to 60% of all volatiles released at the height of emissions (Table S1). The relative proportion of aliphatic compounds increased during the later part of the day and throughout the night (Fig. S1*B*). Absolute emissions of either class of compounds dropped to near-background levels at night, suggesting that their release is influenced by circadian rhythm, light, and/or temperature.

No increase in volatile emission was seen before the onset of the light period between 0500 and 0600 hours (data not shown), and the rhythmic pattern of diurnal emission continued when temperature was kept constant at 22 °C during the light–dark cycles (Fig. S1*C*). To test whether volatile emission is controlled by a circadian rhythm, volatiles were measured over extended dark periods and light periods (Fig. 2 *B* and *C*) beginning after the first day of bloom. The diurnal rhythm of emission was still present after 4 days without light (Fig. 2*B*). Conversely, the pattern of peak emission between 0600 and 1100 hours was lost at constant light (Fig. 2*C*). These results suggest that light, but not temperature, is a critical factor for the rhythmic diurnal emission of volatiles from grapevine flowers, but conditions of constant light disturb this endogenous circadian rhythm.

Volatiles Accumulate in Prebloom Anthers Before Emission at Bloom. Over a 4-day period, we examined whether the rate of volatile emission correlated with the number of flowers open within a flower cluster (Table S2). Flowers were considered open when the caps had fallen off (Fig. 1*B*). No substantial volatile release was detected on the first day, when most flowers were closed. The maximum volatile emission was detected on day 3, when 50% of the flowers were visibly open. Additional flowers may have been already partially open at this time, allowing the release of volatiles before the caps had fallen off, because opening of the cleistogamous flowers of cultivated grapevine often is caused by anthers dehiscing with incomplete loss of caps (15).

To further investigate developmental and spatial patterns of grapevine floral scent formation, we analyzed individual flowering stages defined according to Gribaudo et al. (16) based on visual appearance. We used flowers in prebloom development

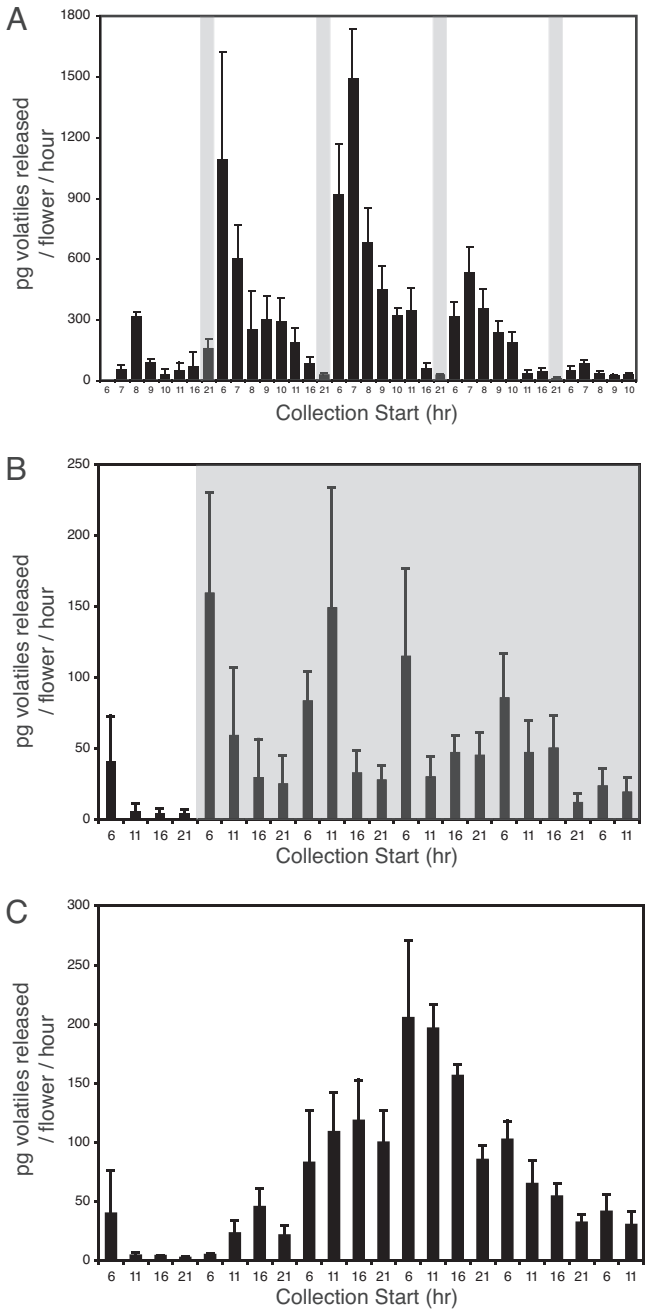

Fig. 2. Time course of volatile emissions from grapevine flowers at bloom. Data represent the amounts of volatiles detected by GCMS. Gray bars illustrate the period of darkness for each experiment. (*A*) Time course of volatile emissions divided into hourly segments between 0600 and 1100 hours. Bars represent 2–6 replicates + SEM. (*B*) Volatile emissions during constant darkness after the first day of blooming. Bars represent 5 replicates + SEM. (*C*) Volatile emissions during constant light conditions. Bars represent 3 replicates + SEM.

stages IV–VI (Fig. 1 *C–E*), at bloom, and at fruit set (Fig. 1*F*). Flowers were dissected into anthers, caps, and pistils, and the individual flower parts were extracted in pentane. Most of the extractable volatile compounds were present in the anthers during prebloom stages V and VI and at bloom (Fig. 3*A*). In contrast, very low amounts of the same compounds were found in other flower parts or in anthers at stage IV and at fruit set. Sesquiterpenes composed a substantial portion of the total extractable compounds from anthers during prebloom stages V

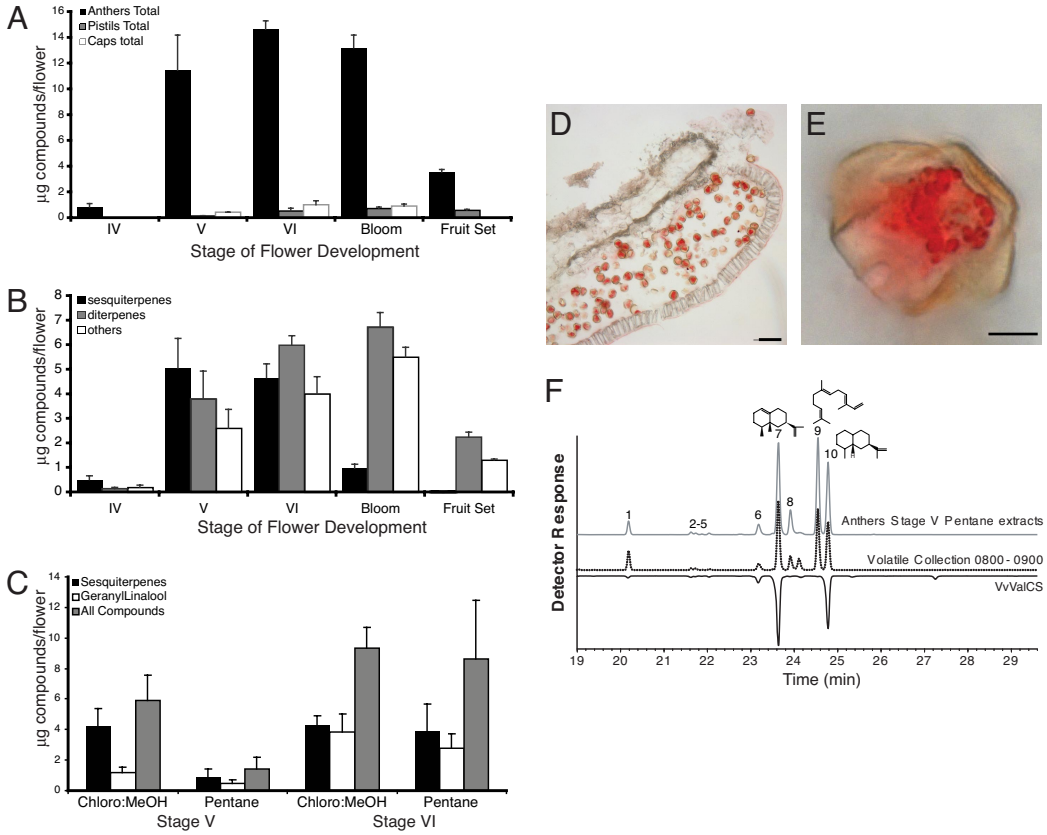

Fig. 3. GCMS analysis of volatile compounds extracted from grapevine flower parts. (*A*) Total pentane-extractable compounds present in anthers, pistils, and caps. Bars represent 4 independent replicate extractions + SEM, with each replicate comprising 10 individual flowers per stage. (*B*) Pentane extracts from anthers analyzed by type of compound present: sesquiterpenes, diterpenes, or aliphatics. Bars represent 4 replicates + SEM. (*C*) Quantitative analysis of the pollen pentane and chloroform/methanol extracts from stage V and VI flowers. Bars represent 4 replicates + SEM. (*D*) Light microscopy image of a stage VI anther stained with Oil Red O. (Scale bar = 100 μm.) (*E*) High-magnification image of a pollen grain showing abundant lipid bodies stained with Oil Red O inside the pollen. (Scale bar = 5 μm.) (*F*) GCMS total ion chromatogram of the products from VvValCS enzyme (solid black line) compared with the anther extracts (solid gray line) and the flower volatile emissions collected on a day of peak release (dashed line). Compounds are as follows: E-β-caryophyllene (1), spirolepechinene (2)*, α-humulene (3), unknown sesquiterpene (4), E-β-farnesene (5), selina-4,11-diene* (6), (+)-valencene (7), tridecanone/cis-α-bergomatene (8), E,E-α-farnesene (9), and (–)-7-epi-α-selinene (10). Tentative designations are labeled with an asterisk. Structures of major compounds shown from left to right include valencene, E,E-α-farnesene, and 7-epi-α-selinene.

and VI, but decreased significantly at bloom and fruit set (Fig. 3*B*). Apparently, the sesquiterpene volatiles were released quickly after flowers and anthers opened. In contrast, aliphatic compounds and diterpenes (one diterpene, geranyllinalool, composed 70%–95% of the diterpenes identified) remained high at bloom and were still present in anthers at fruit set, presumably due to their lower volatility and/or continued biosynthesis of these compounds.

Flower Volatiles in Anthers Are Associated With Pollen Grains and Pollenkitt. To test for the presence of volatiles in the surface pollenkitt or within the pollen grains, we separated pollen from anthers at stages V and VI and extracted volatiles according to the method described by Dobson et al. (17). This method relies on rapid pentane extraction to produce compounds present in the pollenkitt and a longer extraction with chloroform/methanol for compounds present inside the pollen grain. At stage V, most volatiles were found in the chloroform/methanol fraction, indicating that these compounds may be produced inside the pollen grain (Fig. 3*C* and Fig. S2*A*). Analysis of stage VI pollen grains revealed volatiles both inside and outside of the pollen grain. These compounds may be transported to the pollenkitt before anthesis to facilitate volatile release. To visualize lipids that may serve for prebloom sequestration of lipophilic volatiles inside the pollen grain, anthers were cryosectioned and stained with Oil Red O for light microscopy. The images presented in Fig. 3*D* and *E* show dense clusters of lipid bodies (seen as globular red dots) inside the pollen grains.

Valencene Synthase Produces Sequiterpene Volatiles in Grapevine Anthers. In previous work (18), we functionally characterized a cDNA encoding (+)-valencene synthase (*VvValGw*) responsible for producing (+)-valencene and (−)-7-*epi*-α-selinene and 5 minor sesquiterpenes from *V. vinifera* L. cv. Gewürztraminer. Because (+)-valencene and (−)-7-*epi*-α-selinene are 2 of the 3 most abundant sesquiterpenes in the volatile emissions of Cabernet Sauvignon flowers (Table S1), we cloned and functionally characterized *VvValCS* cDNA from Cabernet Sauvignon flowers. The full-length *VvValCS* cDNA contains an ORF of 1,671 nt and encodes a protein of 556 aa. The VvValCS sequence is nearly identical (99% at the nt and aa levels) to VvValGw (Fig. S3). His-tagged VvValCS was expressed in *Escherichia coli*, and the purified sesquiterpene synthase enzyme activity showed the same product profile (Fig. S2*B*), dominated by (+)-valencene and (−)-7-*epi*-α-selinene, as VvValGw with farnesyl diphosphate (FPP) as the substrate. The sesquiterpene products of VvValCS have similar retention time and mass fragmentation patterns as those found in the flower volatile emissions and anther extracts, except for E,E-α-farnesene and an aliphatic methylketone, 2-tridecanone (Fig. 3*F*).

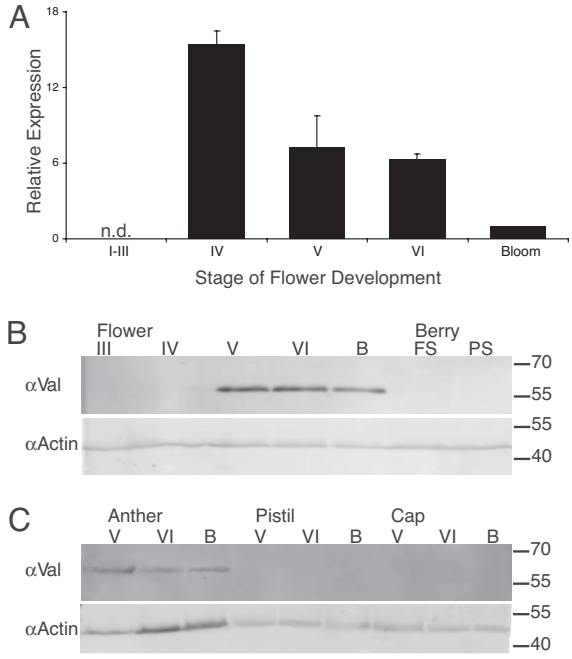

Fig. 4. Stage-specific expression of *VvValCS* gene and VvValCS protein. (*A*) Quantitative RT-PCR analysis of *VvValCS* mRNA during flower development. *VvValCS* transcript abundance is shown at stages I–VI relative to transcript abundance at bloom. Each bar represents measurements from 3 technical replicates for each of 2 biological replicates ± SEM. GAPDH was used as an endogenous control. ΔCt for stages I–III was <2 cycles different from no template controls = no expression. (*B*) Protein expression of VvValCS in flower (stages I—VI and bloom) and berry stages (fs, fruit set; ps, pea size). SDS/PAGE gels were loaded with protein from ≈3 mg of tissue. Actin was measured as a loading control. (*C*) Protein expression of VvValCS in anthers, pistils, and caps at stages V and VI and bloom. Gels were loaded with protein for each flower organ pooled from 15 flowers for each stage of development. Actin was measured as a loading control.

To further substantiate the localization of sequiterpene biosynthesis, we measured sesquiterpene synthase enzyme activity in total protein isolated from anthers. These assays revealed 2 sesquiterpene synthase products, valencene and 7-epi-α-selinene, produced at a rate of 0.184 ± 0.002 and 0.186 ± 0.009 pmol sesquiterpene/mg protein/h, respectively. Neither of these compounds (nor any other sesquiterpene) was detected in the no-substrate or no-enzyme control assays. Sesquiterpene synthase enzyme activity was not detected in protein extracts obtained from any other floral organ. These results support a role for VvValCS in the formation of volatiles in anthers. We did not detect E,E-α-farnesene (the third major sesquiterpene volatile in Cabernet Sauvignon flowers) as a product in these sesquiterpene synthase assays.

***VvValCS* Transcripts Are Most Abundant at Prebloom, Whereas VvVal Protein Accumulates at Prebloom and at Bloom.** To understand how the synthesis of sesquiterpene volatiles is controlled at the transcript level in grapevine flowers, we isolated RNA from inflorescences at all prebloom stages I–VI and at bloom and used quantitative real-time PCR (qRT-PCR) to measure *VvValCS* transcript abundance. Whereas *VvValCS* transcripts were below the detection limit at stages I–III (Ct values < -2 no template control Ct), transcript abundance dramatically increased at stage IV (Fig. 4*A*), followed by a decrease at stages V and VI and at bloom.

To complement transcript analysis with protein detection, we used a polyclonal antibody raised against a 15-aa synthetic peptide (Fig. S3) from VvVal. The antibody gave single bands of the correct molecular weight when tested in immunoblotting with recombinant VvValGw and VvValCS protein (Fig. S4*A*). Anti-VvVal did not give signals in Western blotting when tested against 11 other grapevine recombinant terpene synthases (data not shown). VvVal protein was detected at prebloom stages V and VI and, to a slightly lesser extent, at bloom (Fig. 4*B*). VvVal was not detected at any of the other flower or berry stages or in roots, seeds, or leaves (Fig. S4 *B* and *C*). The results from VvVal protein measurements over the developmental time course are consistent with the presence of the sesquiterpene products from VvVal enzyme activity in stage V and stage VI flowers (Fig. 3 *B* and *C*), which is preceded by the peak of *VvVal* transcripts at stage IV (Fig. 4*A*).

To localize VvVal during flower development, we dissected flowers into anthers, pistils, and sepals during stages V and VI and bloom. Immunoblot analysis demonstrated the presence of VvVal in the protein isolated from anthers, but not in that isolated from pistils or caps (Fig. 4*C*).

VvVal Is Localized Within Pollen Grains. Based on the detection of VvVal in anthers at stages V and VI and bloom (Fig. 4*C*), we investigated VvVal localization at the level of specific tissue or cell type. For the immunohistochemical analyses, we used VvVal antibody in combination with Alexa-488 secondary antibody and fluorescent microscopy on resin-embedded flower samples at 6 developmental stages (II–VI and bloom) to visualize VvVal within flower tissues. Sections of the resin-embedded samples were labeled with either VvVal antibody or preimmune serum. Floral tissues had a considerable amount of autofluorescence in both channels. Autofluorescence was particularly strong in pollen grains, as reported previously (19).

Consistent with the immunoblot analyses, VvVal was not detected by immunohistochemical in situ analysis at the early prebloom stages II–IV (data not shown), whereas sections from stages V and VI showed discrete areas of punctuate fluorescence signals in the presence of VvVal antibody localized to the inside of pollen grains (Fig. 5 *B* and *D* and Fig. S5 *A* and *C*). The VvVal-specific fluorescence signal was localized primarily around spherical bodies within the pollen grain (Fig. 5 *D* and Fig. S5 *C*). No such signal was found in sections treated with preimmune serum instead of VvVal antibody (Fig. 5 *C* and *E* and Fig. S5 *B* and *D*) and in no–primary antibody controls. Some additional fluorescence signal localized VvVal to the intine/exine region of several pollen grains at stages V and VI (Fig. 5 *B* and *D* and Fig. S5 *C*). No substantial signal was seen between the pollen grains (inside the locule of the anther), and little label was detected on the outside of the pollen grains, suggesting that VvVal protein is localized primarily to the inside of the pollen grains, not to disintegrating tapetum cells or the pollenkitt. In addition, no signal was seen in the cells composing the anthers and filaments.

When visualized under high magnification (63×), sections treated with anti-VvVal revealed clusters of punctate signals around the outside of spherical bodies. Whereas pollen grains have a number of distinct organelles and subcellular structures such as lipid bodies, plastids, and vacuoles (20), these spherical bodies likely are lipid vesicles similar to those identified by light microscopy with Oil Red O staining (Fig. 3 *D* and *E*). This observation is supported by visualization of anti-VvVal immunolabeling using TEM (Fig. 6 *A–F* and Fig. S6 *A–F*). TEM revealed stage VI flowers with substantial amounts of anti-VvVal label localized primarily at the outer edges of individual or merging lipid vesicles. No label was seen in the control, and very little label was seen in other portions of the pollen grain.

Discussion

Using several lines of evidence, including results from metabolite analysis of headspace volatile collections and anther and pollen extracts, VvValCS enzyme activity assays, and VvValCS protein localization, we have shown that anthers—more specifically,

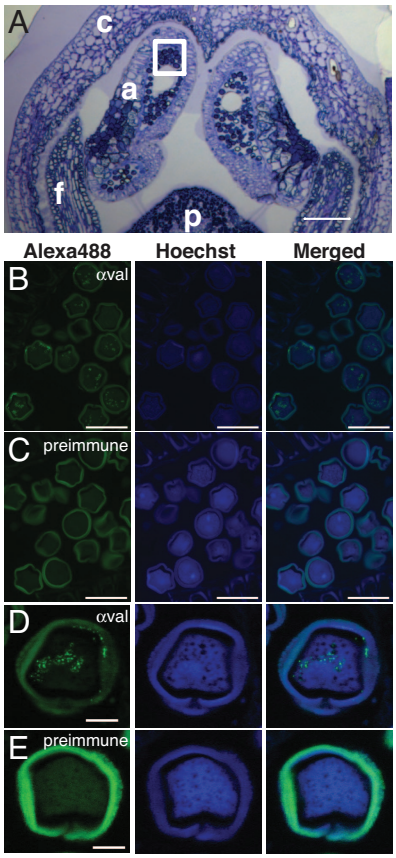

Fig. 5. Immunofluorescence localization of VvValCS protein to the pollen grains of stage V flowers. (*A*) Longitudinal section of a grape flower (f) stained with toluidine blue. The box highlights the portion of the anther (a) imaged in (*B–M*). The pistil (p) and the cap (c) are indicated in white. (Scale bar = 200 μm.) (*B–E*) The first column of images shows fluorescence from VvVal primary antibody with Alexa-488 secondary, the second column shows the same section with 332 Hoechst staining of nuclei, and the third column shows the 2 channels overlaid. VvVal is seen in the images with discrete green clusters. Diffuse autofluoresence is present for the blue and green channels for all treatments. (*B* and *C*) Images of a section of an anther locule containing pollen grains. VvVal is localized primary inside the stage V pollen grains. Some label is found on the edges of the pollen grains. Little label is found on the outside of the pollen grains or in other parts of the anther locule. (Scale bar = 50 μm.) (*D* and *E*) High-magnification (63×) images of representative pollen grains from stages V. Most of the label is present within the pollen grain, although some label is seen on the inner edges of the pollen grains as well. (Scale bar = 10 μm.)

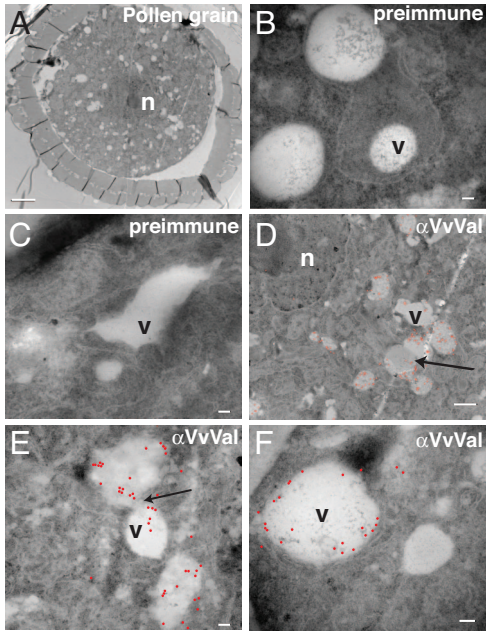

Fig. 6. TEM immunogold localization of VvVal within pollen grains. (*A*) Pollen grain with a single nucleus (n). (Scale bar = 2 μm.) (*B–F*) Pollen grain sections with lipid vesicles (v). Arrows indicate fusions of vesicles. Immunogold labeling of α-VvVal primary is highlighted in red after imaging; the original image is provided for reference as a supplementary figure. Most of the label is present on the outer edges of these lipid vesicles. No label is seen in the preimmune control. [Scale bar = 500 nm for (*B*), (*C*), (*E*), and (*F*) and 100 nm for (*D*).].

pollen grains—are the site of sesquiterpene volatile synthesis in grapevine flowers. The presence of these volatiles precedes flower opening. Gene expression analysis found that the highest transcript abundance for *VvValCS* is from stage IV flowers, preceding the peak of VvValCS protein and the presence of volatile compounds. Whereas VvValCS accounts for 2 of the 3 major grapevine flower volatiles, the enzyme for E,E-α-farnesene synthesis remains to be identified in the numerous terpene synthases in the grapevine genome (21, 22).

Immunofluorescence analysis throughout flower development showed VvValCS protein clearly localized within pollen grains, and transmission electron microscopy (TEM) localized VvValCS with the outer edge of lipid vesicles, which are abundant in the maturing microspore but no longer seen at anthesis. Whereas tapetum cells have been attributed to the production of lipids, phenylpropanoids, proteins, carbohydrates, and carotenoids, which eventually compose the pollenkitt or pollen coat (4, 5, 23), our results do not support a role of tapetum cells in the ontogenesis of sesquiterpene volatiles, which seems to arise primarily from VvValCS in the developing microspores. The biosynthesis of terpene volatiles within anthers and pollen grains before bloom presents a substantially different biological system of floral scent formation than those described from species studied previously, in which floral scent biosynthesis occurs during the blooming process and is been attributed to other flower tissues but not the male flower parts (12).

Materials and Methods

Plant Material. *V. vinifera* L. cv. Cabernet Sauvignon canes (clone 15 grafted on rootstock 101–14) containing 6 nodes were harvested from Bull Pine Estate Vineyards (Vincor), Osoyoos, BC in January 2007 and 2008 and kept at 4 °C before rooting. Plants were grown as described by Mullins and Rajasekaran (24) with some modifications, as detailed in *SI Materials and Methods*.

Volatile Collection. An automated volatile collection system (Analytical Research Systems) was used as described previously (25). Details are given in *SI Materials and Methods*.

Flower and Pollen Extractions. For each stage (V to bloom), 10 flowers were separated into anthers, caps, and pistils/pedicels, and the individual flower parts were immediately submerged in 0.5 mL of pentane containing 2.0 μg/mL of isobutylbenzene as an internal standard. Volatiles were directly extracted from pollen grains using the method specified by Dobson et al. (17) with modifications, as described in *SI Materials and Methods*.

GCMS Analysis. GCMS analysis was performed as described previously (26). Details are provided in *SI Materials and Methods*.

VvValCS cDNA Cloning and Recombinant Protein Enzyme Assays. RNA was extracted from flowers, and cDNA was made as described by Reid et al. (27). *VvValCS* cDNA was isolated by PCR using primers designed against the TIGR contig TC38950. *VvValCS* and the previously described *VvValGw* (18) were cloned into pET28b(+) (Novagen) and expressed as C-terminal His-tag fusion proteins in *E. coli* C41 cells containing the pRARE 2 plasmid (28). Single-vial assays were used for functional characterization, as described previously (28, 29). Additional details are provided in *SI Materials and Methods*.

Enzyme Assays With Protein from Anthers. Anthers were dissected from 100 stage VI flowers, frozen in liquid nitrogen, and ground with sea sand in a mortar and pestle for 5 min. Then 5 mL of extraction buffer [50 mM Tris (pH 7.5), 10% polyvinylpolypyrrolidone (wt/vol), 1% polyvinylpyrrolidone-40 (wt/vol), 2 mM DTT, 0.2% activated charcoal, 10% (wt/vol) glycerol, and 1 mM PMSF] was added. Extracts were sonicated using a Branson digital sonifier at 15% power for 1 min on ice, and then ground with a mortar and pestle for another 5 min. The extract containing soluble protein was centrifuged at 3500 $\times$ *g* for 30 min at 4 °C. Supernatant was further cleared at 21,000 $\times$ *g* for 30 min at 4 °C and desalted using PD MiniTrap G-10 columns (GE Healthcare Life Sciences). Enzyme assays were performed as described for recombinant enzyme assays, but with 0.25 mL of desalted protein extract (0.65 mg protein/mL) used for each assay. Controls included assays without substrate or without protein.

Protein Extraction for Western Blot Analysis. Protein from individual flowers was extracted by resuspending powdered frozen plant tissue in loading buffer. For floral organs, total protein was extracted as described by Holmes-Davis et al. (30). These procedures are detailed in SI *Materials and Methods*.

Immunoblot Analysis. Immunoblot analyses followed standard procedures using polyclonal VvVal antibodies made against a synthetic peptide (EDLKKEVKRKLTAAC) by Sigma-Genosys (Sigma-Aldrich). Details of the methods are provided in *SI Materials and Methods*.

Immunohistochemistry and Fluorescence Microscopy. Flower tissues were fixed and embedded as described previously (31), and immunolabeling using α-VvVal was done following standard procedures, as described in detail in *SI Materials and Methods*. Fluorescence microscopy was done using an AxioVert 200M and an AxioImager Z1 fitted with an Apotome (Carl Zeiss). Alexa 488 was imaged using an EndowGFP bandpass filter (#41017; Chroma Technology), and 332 Hoechst nuclei staining was imaged with an AMCA filter (#31000; Chroma Technology). All images were analyzed using AxioVision 4.7 (Carl Zeiss).

TEM. Resin-embedded sections that gave signals for VvVal localization were resectioned using an ultra-diamond knife (50 nm thick) and then adhered to formvar-coated nickel grids. Immunolabeling was done as described above but using 5% BSA instead of skim milk, and all TBST buffers were filtered through a 0.22-μm filter before use. Secondary labeling was done with 10-nm gold goat anti-rabbit (British Biocell). TEM imaging was performed using a Hitachi H7600 transmission electron microscope operating at 80–100 kV.

Light Microscopy. Stage VI anthers were embedded and frozen in OCT medium before being cryosectioned at a thickness of 25 μm. Sections were melted onto a slide, fixed for 10 min in 4% paraformaldehyde, and stained with Oil Red O (0.1 g of Oil Red O in 60% isopropanol) for 15 min. After a rinse with 60% isopropanol, the sections were covered with mounting medium and visualized by light microscopy.

qRT-PCR. Flowers at stages I–VI and bloom were used for RNA isolation, cDNA synthesis, and comparative Ct RT-PCR analysis as described by Reid et al. (27). Details are provided in *SI Materials and Methods*.

ACKNOWLEDGMENTS. We thank Dr. Oliver Prange for helpful discussions and microscopy assistance, the Alaa El-Husseini Laboratory for the generous use of their microscopes, and Vincor Canada for access to their vineyards for cane collection. This research was supported by grants from Genome Canada and Genome British Columbia (to J.B. and S.T.L.) and the Natural Sciences and Engineering Research Council of Canada (postdoctoral fellowship to D.M.M.; discovery grant and E.W.R. Steacie Memorial Fellowship to J.B.). J.B. is a University of British Columbia Distinguished Scholar.

1. Dobson HEM, Bergstroem G (2000) The ecology and evolution of pollen odors. *Plant Syst Evol* 222:63–87.
2. Pellmyr O, Thien LB (1986) Insect reproduction and floral fragrances. *Taxon* 35:76–85.
3. Ashman T-L, Cole DH, Bradburn M, Blaney B, Raguso RA (2005) The scent of a male. *Ecology* 86:2099–2105.
4. Pacini E, Hesse M (2005) Pollenkitt: Its composition, forms and functions. *Flora (Jena)* 200:399–415.
5. Piffanelli P, Ross JHE, Murphy DJ (1998) Biogenesis and function of the lipidic structures of pollen grains. *Sex Plant Reprod* 11:65–80.
6. May P (2000) From bud to berry, with special reference to inflorescence and bunch morphology in *Vitis vinifera* L. *Aust J Grape Wine Res* 6:82–98.
7. Carmona MJ, Chaib J, Martinez-Zapater JM, Thomas MR (2008) A molecular genetic perspective of reproductive development in grapevine. *J Exp Bot* 59:2579–2596.
8. Kimura PH, Okamoto G, Hirano K (1998) The mode of pollination and stigma receptivity in *Vitis coignetiae* Pulliat. *Am J Enol Viticult* 49:1–5.
9. Buchbauer G, Jirovetz L, Wasicky M, Herlitschka A (1994) Headspace analysis of *Vitis vinifera* (Vitaceae) flowers. *J Essent Oil Res* 6:313–314.
10. Buchbauer G, Jirovetz L, Wasicky M, Herlitschka A, Nikiforov A (1994) Aroma of white wine flowers. *Z Lebensm Unters Forsch* 199:1–4 (in German).
11. Buchbauer G, Jirovetz L, Wasicky M, Nikiforov A (1995) Aroma from red wine flowers. *Z Lebensm Unters Forsch* 200:443–446 (in German).
12. Dudareva N, Pichersky E (2006) in *Biology of Floral Scent*, eds Dudareva N, Pichersky E (CRC Press, Boca Raton, FL), pp. 55–78.
13. Lee S, Chappell J (2008) Biochemical and genomic characterization of terpene synthases in *Magnolia grandiflora*. *Plant Physiol* 147:1017–1033.
14. Mandaokar A, Kumar VD, Amway M, Browse J (2003) Microarray and differential display identify genes involved in jasmonate-dependent anther development. *Plant Mol Biol* 52:775–786.
15. Staudt G (1999) Opening of flowers and time of anthesis in grapevines, *Vitis vinifera* L. *Vitis* 38:15–20.
16. Gribaudo I, Gambino G, Vallania R (2004) Somatic embryogenesis from grapevine anthers. *Am J Enol Viticult* 55:427–430.
17. Dobson HEM, Bergstroem G, Groth I (1990) Differences in fragrance chemistry between flower parts of *Rosa rugosa* Thunb. (Rosaceae). *Isr J Bot* 39:143–156.
18. Lücker J, Bowen P, Bohlmann J (2004) *Vitis vinifera* terpenoid cyclases. *Phytochemistry* 65:2649–2659.
19. Zhang XY, et al. (2006) A shift of phloem unloading from symplasmic to apoplasmic pathway is involved in developmental onset of ripening in grape berry. *Plant Physiol* 142:220–232.
20. Pacini E (2000) From anther and pollen ripening to pollen presentation. *Plant Syst Evol* 222:19–43.
21. French-Italian Public Consortium for Grapevine Genome Characterization (2007) The grapevine genome sequence suggests ancestral hexaploidization in major angiosperm phyla. *Nature* 449:463–467.
22. Velasco R, et al. (2007) A high-quality draft consensus sequence of the genome of a heterozygous grapevine variety. *PLoS ONE* 2:e3107.
23. Wang A, et al. (2002) Male gametophyte development in bread wheat (*Triticum aestivum* L.). *Plant J* 30:613–623.
24. Mullins MG, Rajasekaran K (1981) Fruiting cuttings: Revised method for producing test-plants of grapevine cultivars. *Am J Enol Viticult* 32:35–40.
25. Arimura G, Huber DP, Bohlmann J (2004) Forest tent caterpillars (*Malacosoma disstria*) induce local and systemic diurnal emissions of terpenoid volatiles in hybrid poplar (*Populus trichocarpa x deltoides*). *Plant J* 37:603–616.
26. Martin DM, Gershenzon J, Bohlmann J (2003) Induction of volatile terpene biosynthesis and diurnal emission by methyl jasmonate in foliage of Norway spruce. *Plant Physiol* 132:1586–1599.
27. Reid KE, Olsson N, Schlosser J, Peng F, Lund ST (2006) An optimized grapevine RNA isolation procedure and statistical determination of reference genes for real-time RT-PCR during berry development. *BMC Plant Biol* 6:27.
28. Keeling CI, Weisshaar S, Lin RP, Bohlmann J (2008) Functional plasticity of paralogous diterpene synthases involved in conifer defense. *Proc Natl Acad Sci USA* 105:1085–1090.
29. O'Maille PE, Chappell J, Noel JP (2004) A single-vial analytical and quantitative gas chromatography–mass spectrometry assay for terpene synthases. *Anal Biochem* 335:210–217.
30. Holmes-Davis R, Tanaka CK, Vensel WH, Hurkman WJ, McCormick S (2005) Proteome mapping of mature pollen of *Arabidopsis thaliana*. *Proteomics* 5:4864–4884.
31. Hudgins JW, Ralph SG, Franceschi VR, Bohlmann J (2006) Ethylene in induced conifer defense. *Planta* 224:865–877.